ChemInform Abstract: 1/∞[ZrPSe6−]: A Soluble Photoluminescent Inorganic Polymer and Strong Second Harmonic Generation Response of Its Alkali Salts

ARTICLE *in* JOURNAL OF THE AMERICAN CHEMICAL SOCIETY · OCTOBER 2008

Impact Factor: 12.11 · DOI: 10.1021/ja804166m · Source: PubMed

J|A|C|S
COMMUNICATIONS

Published on Web 08/21/2008

$^1/_\infty[ZrPSe_6^-]$: A Soluble Photoluminescent Inorganic Polymer and Strong Second Harmonic Generation Response of Its Alkali Salts

Santanu Banerjee,[†] Christos D. Malliakas,[†] Joon I. Jang,[§] John B. Ketterson,[§] and Mercouri G. Kanatzidis*[,†,‡]

Department of Chemistry, Northwestern University, Evanston, Illinois 60208, Materials Science Division, Argonne National Laboratory, Argonne, Illinois 60439, and Department of Physics and Astronomy, Northwestern University, Evanston, Illinois 60208

Received June 2, 2008; E-mail: m-kanatzidis@northwestern.edu

The class of metal chalcophosphates exhibits wide structural diversity and technologically promising properties such as ferroelectricity,[1−4] nonlinear optical behavior,[5−7] photoluminescence,[8] and phase change.[9] In part, the structural diversity arises from the broad variety of anions including $^1/_\infty[P_2Se_6^{2-}]$,[7b] $[PQ_4]^{3-}$,[10] $[P_2Se_9]^{4-}$,[11] $[P_2Q_6]^{4-}$,[12] $[P_2Q_{10}]^{4-}$,[13] $[P_8Se_{18}]^{4-}$,[14] $[P_6Se_{12}]^{4-}$,[15] and $^1/_\infty[PSe_6]^{-}$[16] (Q = S, Se). The preponderance of these species has been synthesized with the molten flux technique.[17−19]

The chalcophosphates may be a good source of nonlinear optical (NLO) materials because the noncentrosymmetric structural motif is common in this family.[7b] In addition, the idea of using the d^0 metal ions (e.g., Ti^{4+}, Nb^{5+}, Mo^{6+}, etc.) to obtain noncentrosymmetric arrangements due to second-order Jahn−Teller distortions has been proposed.[20] Here we investigated the selenophosphate chemistry of the d^0 metal ion, Zr^{4+}. Alkali metal salts of a novel quaternary zirconium selenophosphate phase were isolated using the molten flux technique, having a general formula of $AZrPSe_6$ [A = K(**1**), Rb(**2**), Cs(**3**)].[21] To the best of our knowledge, this is the first quaternary zirconium selenophosphate phase structurally characterized to date.

All three salts of $AZrPSe_6$ have a highly anisotropic structure based on the polymeric chain of $^1/_\infty[ZrPSe_6^-]$. They are semiconductors with high transparency over most of the infrared spectrum. Because of the noncentrosymmetric structure consisting of highly polarizable, covalently bonded P and Se atoms, the $AZrPSe_6$ compounds exhibit a strong second harmonic generation (SHG) response. The Cs analogue showed the highest SHG intensity which is ∼15× stronger than that of $AgGaSe_2$, a benchmark NLO material used commercially.[22] The $AZrPSe_6$ compounds are soluble in hydrazine and show blue-shifted optical absorption and strong room temperature photoluminescence. The solubility makes them promising candidates for solution processing.

The structural characterization of $AZrPSe_6$ was very challenging because the intrinsic tendency of these systems is to crystallize as microneedles. Upon exploring numerous heating profiles and temperatures, pure compounds could be isolated as very tiny, needle-shaped single crystals (Figure 1A), which we could structurally characterize using only Synchrotron radiation (Advanced Photon Source, Argonne National Laboratory).

The new compounds $AZrPSe_6$ [A = K (**1**), Rb (**2**), Cs (**3**)] crystallize in the polar space group $Pmc2_1$.[23] Because all three salts are isostructural, this discussion will mainly focus on the K-salt which features parallel chains of the infinite $^1/_\infty[ZrPSe_6^-]$ anion

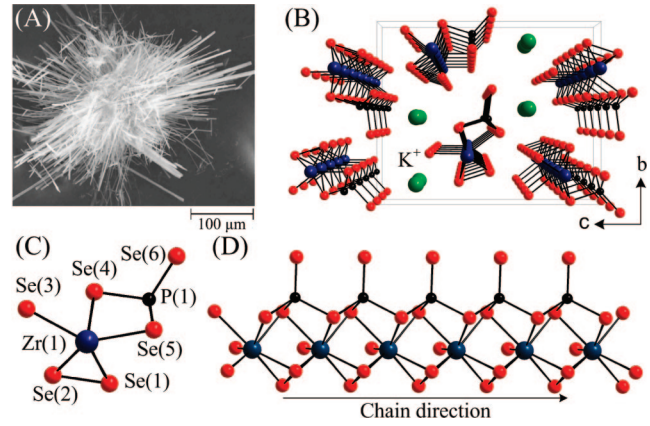

Figure 1. (A) SEM image of needle shaped microcrystal of $KZrPSe_6$ (**1**). (B) Noncentrosymmetric structure of **1**: Molecular view along the [100] direction. (C) View of $[ZrPSe_6]^-$ anion along the chain axis. (D) Polymeric $^1/_\infty[PSe_3^-]$ chain acting as a backbone holding the Zr^{4+} ions together.

separated by the alkali metal ions (Figure 1B). The chains have Zr^{4+} ions coordinated to Se atoms in a distorted bicapped trigonal prismatic geometry (Figure 1C). All Zr^{4+} ions are connected to a $^1/_\infty[PSe_3^-]$ polymeric backbone formed by the condensation of corner-sharing tetrahedral PSe_4 units (Figure 1D). Each phosphorus atom has a terminal P−Se bond projecting out from the one-dimensional chain structure. The Zr atoms are also bridged with η^4-bonded Se_2^{2-} groups. Finally, there is also terminal Se(3) atom on each zirconium metal center.

The PSe_4 tetrahedron is distorted from the ideal geometry having Se−P−Se angles ranging from 99.382(14)° to 114.975(9)°. The P−Se bonds are of two different lengths, as three in the PSe_4 group are engaged in forming the polymeric backbone and one is terminal. All the P−Se bond lengths are normal, the bridging ones [P(1)−Se(4), P(1)−Se(5)] being at 2.245(1)−2.277(1) Å and the terminal [P(1)−Se(6)] at 2.108(1) Å. The Se−Se bond length in Se_2^{2-} is 2.3515(90) Å.

The Zr^{4+} metal ion is bonded to three different sets of Se atoms. The bonds with two bridging selenium atoms [Zr(1)−Se(4) and Zr(1)−Se(5)] from the PSe_4 group are at 2.782(3)−2.797(6) Å, whereas those from the Se_2^{2-} group [Zr(1)−Se(1) and Zr(1)−Se(2)] are shorter at 2.697(4) Å. The intrachain Zr−Zr distances are at 3.708(1) Å. Interestingly the $AHfPSe_6$ [A = Rb, Cs] analogues are also stable featuring the same chains but different crystal packing. The $AZrPSe_6$ compounds are only the second example of a polymeric selenophosphate anion being coordinated to a transition metal, the first one being $K_3RuP_5Se_{10}$ which contains a different polymer.[24]

[†] Department of Chemistry, Northwestern University.
[‡] Argonne National Laboratory.
[§] Department of Physics and Astronomy, Northwestern University.

10.1021/ja804166m CCC: $40.75

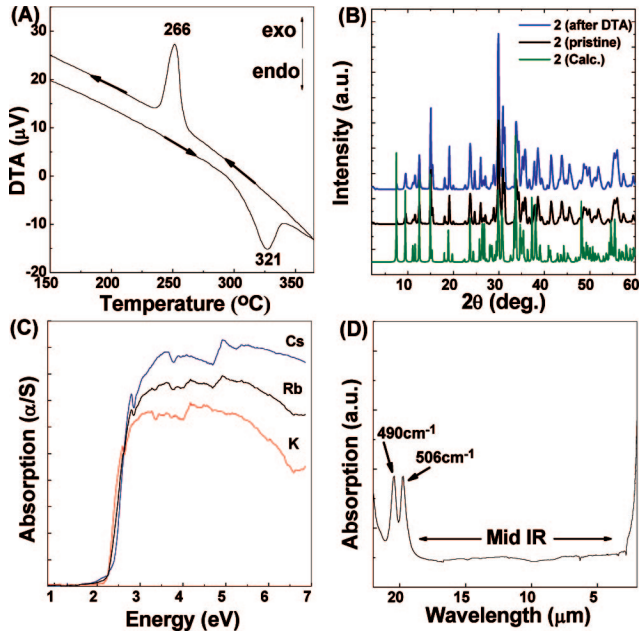

Figure 2. (A) DTA plot of $RbZrPSe_6$. (B) X-ray powder patterns of $RbZrPSe_6$ before and after DTA, compared with the calculated pattern of **2**. (C) Solid-state UV−vis optical absorption spectra of $AZrPSe_6$ compounds. (D) Far-IR−mid-IR−UV−vis absorption spectra of crystalline **2**.

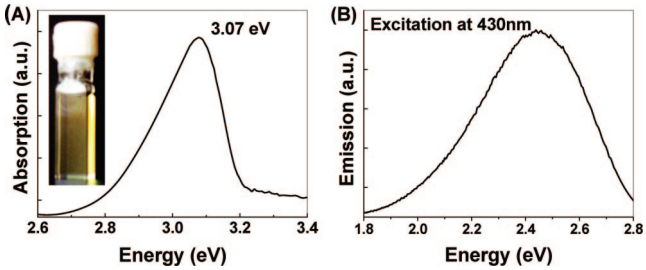

Figure 3. (A) Solution UV−vis absorption of **2** (Inset: Hydrazine solution of **2** in a cuvette). (B) Solution photoluminescence spectrum of **2**.

Differential thermal analysis (DTA) performed on $RbZrPSe_6$ (**2**) at a rate of 10 °C/min showed that it melts at 321 °C and recrystallizes without change upon cooling at 266 °C (Figure 2A). The X-ray powder pattern recorded before and after DTA indicated full recovery of the compound (Figure 2B).

The solid state electronic absorption spectra for compounds **1**, **2**, and **3** (Figure 2C) showed very strong and sharp absorption edges at ∼2 eV. In general, changes in the alkali metal do not show a major effect on the band gap of the covalent network, mainly because of the nondirectional ionic bonding.

The compounds **1**, **2**, and **3** show optical transparency over a wide range starting from the long-wave IR to near IR/visible region of the spectrum. Figure 2D shows that almost no absorption occurs for compound **2** within the range 472 cm^{-1} (18.5 μm) to 4000 cm^{-1} (2 μm). As a comparison, the commercially used NLO material $AgGaSe_2$ is transparent up to 17 μm. The absorption peaks that appear above 18.5 μm correspond to Zr−Se and P−Se stretching modes of the compounds. Optical transparency in the infrared region is required for NLO materials to be used in applications.[22]

Compounds **1**, **2**, and **3** are soluble in hydrazine (∼0.4 mol/L) to form yellow colored solutions with the same optical absorption maximum at 3.07 eV (Figure 3A). The solutions of all compounds showed strong photoluminescence at room temperature when

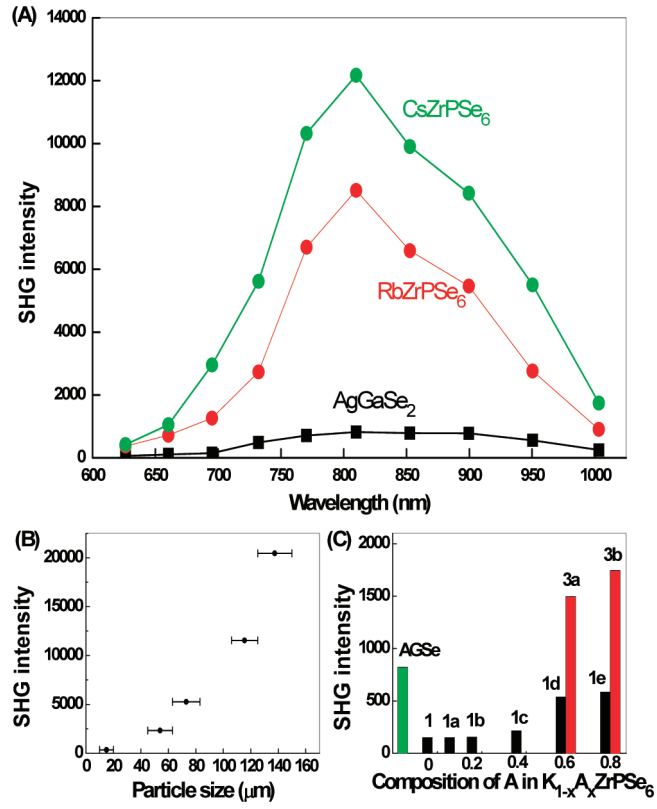

Figure 4. (A) SHG intensity (arbitrary unit) of $CsZrPSe_6$ (**3**) and $RbZrPSe_6$ (**2**) relative to $AgGaSe_2$ over a wide wavelength range. (B) Particle size to SHG intensities diagram for $CsZrPSe_6$. (C) SHG intensities of the solid solutions (**1a**−**e**, **3a**−**b**) compared with **1** and $AgGaSe_2$.

excited above the band gap energy (430 nm) as shown in Figure 3B. Both the absorption and photoluminescence spectra are believed to originate from completely dispersed $^1/_\infty[ZrPSe_6^-]$ chains. The Stokes shift of ∼0.6 eV observed is similar to those of conjugated polymers.[25] To our best knowledge this is the first example of a light-emitting selenophosphate species.

Solution ^{31}P NMR spectra were recorded for the hydrazine solutions using 85% phosphoric acid as the standard. For all compounds a singlet peak was observed at ∼30.5 ppm.[21] The NMR chemical shift mainly depends on the degree of local symmetry around the phosphorus atom.[26] The $RbPSe_6$[19] compound showed a shift around 4.3 ppm in the solid state, whereas **2** shows a shift around 30 ppm. The difference can be attributed to the coordination of the asymmetric PSe_4 group to the highly electropositive Zr^{4+} cation in the latter. Also the PSe_4 group coordinated to W^{4+} in $[W(PSe_4)(PSe_2)(Se)]^{2-}$ showed a positive shift of 10.89 ppm in the ^{31}P NMR spectrum.[27] The ^{31}P NMR results suggest that, upon dissolution, the chains retain their compositional integrity. The polar nature of the title compounds along with their good solution properties suggests that they may be promising candidates for solution processing of NLO films.[28]

The polar structure of $AZrPSe_6$ causes all three compounds (**1**−**3**) to show a significant NLO response. The SHG response was measured for compounds **1**−**3** following the modified Kurtz powder method[29] using an infrared light source tunable from 1000 to 2000 nm. All samples were of the same particle size (45−63 μm) and prepared under similar conditions, and their SHG signal intensities were compared at the same time with $AgGaSe_2$ particles of similar size. The SHG signals from the fundamental idler beam for all three compounds (**1**−**3**) show a maximum around 820 nm (Figure 4A). Among the three salts, the cesium analogue (compound **3**) showed

the strongest SHG intensity presumably due to the largest size and highest polarizability. Under similar experimental conditions the $AgGaSe_2$ response showed an SHG maximum around 820 nm, whereas the SHG response of crystalline **3** and **2** were ~15- and 10-fold stronger at the same wavelength. The K analogue (compound **1**) showed a weaker SHG signal intensity than $AgGaSe_2$. Phase matching experiments performed using different size particles of compound **3** indicate the material to be type I phase matchable (Figure 4B). For practical NLO applications phase matching is necessary.[22] The optical transparency found over a wide range of the spectrum along with the strong SHG response of compounds **2** and **3** makes them promising for thin film infrared NLO applications.[30]

Because the SHG property follows the polarizability trend Cs > Rb > K, series of solid solutions of compounds **1**−**3** were synthesized by doping fractional amounts of more polarizable Rb^+, Cs^+ ions into compound **1**. The SHG signal intensities were measured for nominally prepared samples of compounds **1a** [$K_{0.9}Rb_{0.1}ZrPSe_6$], **1b** [$K_{0.8}Rb_{0.2}ZrPSe_6$], **1c** [$K_{0.6}Rb_{0.4}ZrPSe_6$], **1d** [$K_{0.4}Rb_{0.6}ZrPSe_6$], **1e** [$K_{0.2}Rb_{0.8}ZrPSe_6$], **3a** [$K_{0.4}Cs_{0.6}ZrPSe_6$], and **3b** [$K_{0.2}Cs_{0.8}ZrPSe_6$]. These were compared with $AgGaSe_2$ of the same particle size (45−63 μm) under similar conditions. The relative SHG intensities for **1a**−**e** and **3a**−**b** are shown in Figure 4C. These results confirm that the alkali metal polarizability trend is really correlated to SHG efficiency. A similar observation was reported with $KTiOPO_4/K_{0.5}Rb_{0.5}TiOPO_4$ and $KTiOAsO_4/K_{0.5}Cs_{0.5}TiOAsO_4$[31] and was attributed to the effect of size and polarizability of the alkali metal ions.

In conclusion, the $AZrPSe_6$ [A = K, Rb, Cs] compounds have a unique polar structure featuring chains of $^1/_\infty[ZrPSe_6^-]$. These materials also show wide transparency in the mid-IR region up to 18.5 μm. The polar structure and presence of highly polarizable atoms such as Se, Rb, Cs, Zr result in strong SHG response which is significantly larger than that of the commercial NLO material $AgGaSe_2$. In solution, the chains photoluminesce strongly when excited above the energy gap. Light emission is unprecedented for a selenophosphate species and is reminiscent of the solution behavior of conjugated polymer chains. The high solubility of these compounds in hydrazine is an important property because it makes them promising for future solution processing studies of useful forms, e.g., thin films.

Acknowledgment. Financial support from the National Science Foundation (NSF) (DMR-0801855) is gratefully acknowledged. ChemMatCARS Sector 15 is principally supported by the NSF/Department of Energy (DOE) under Grant Number CHE-0535644. The Advanced Photon Source at Argonne National Laboratory is supported by the DOE, Office of Science, Office of Basic Energy Sciences, Contract No. DE-AC02-06CH11357.

Supporting Information Available: X-ray crystallographic file (in CIF format) as well as tables for structural information. This material is available free of charge via the Internet at http://pubs.acs.org.

References

(1) Carpentier, C. D.; Nitsche, R. *Mater. Res. Bull.* **1974**, *9*, 1097–1100.
(2) Bourdon, X.; Maisonneuve, V.; Cajipe, V. B.; Payen, C.; Fischer, J. E. *J. Alloys Compd.* **1999**, *283*, 122–127.
(3) Rogach, E. D.; Sviridov, E. V.; Arnautova, E. A.; Savchenko, E. A.; Prosenko, N. P. *Zh. Tekh. Fiz.* **1991**, *61*, 201–204.
(4) Scott, B.; Pressprich, M.; Willet, R. D.; Cleary, D. A. *J. Solid State Chem.* **1992**, *96*, 294–300.
(5) (a) Clement, R.; Lacroix, P. G.; Ohare, D.; Evans, J. *Adv. Mater.* **1994**, *6*, 794–797. (b) Lacroix, P. G.; Clement, R.; Nakatani, K.; Zyss, J.; Ledoux, I. *Science* **1994**, *263*, 658–660.
(6) Misuryaev, T. V.; Murzina, T. V.; Aktsipetrov, O. A.; Sherstyuk, N. E.; Cajipe, V. B.; Bourdon, X. *Solid State Commun.* **2000**, *115*, 605–608.
(7) (a) Liao, J. H.; Marking, G. M.; Hsu, K. F.; Matsushita, Y.; Ewbank, M. D.; Borwick, R.; Cunningham, P.; Rosker, M. J.; Kanatzidis, M. G. *J. Am. Chem. Soc.* **2003**, *125*, 9484–9493. (b) Chung, I.; Malliakas, C. D.; Jang, J. I.; Canlas, C. G.; Weliky, D. P.; Kanatzidis, M. G. *J. Am. Chem. Soc.* **2007**, *129*, 14996–15006.
(8) Huang, Z. L.; Cajipe, V. B.; Lerolland, B.; Colombet, P.; Schipper, W. J.; Blasse, G. *Eur. J. Solid State Inorg. Chem* **1992**, *29*, 1133–1144.
(9) (a) Ohta, T.; Nishiuchi, K.; Narumi, K.; Kitaoka, Y.; Ishibashi, H.; Yamada, N.; Kozaki, T. *Jpn. J. Appl. Phys. Part 1* **2000**, *39*, 770–774. (b) Ohta, T. *J. Optoelectron. Adv. Mat.* **2001**, *3*, 609–626. (c) Oh, H.-R.; Cho, B.-H.; Cho, W. Y.; Kang, S.; Choi, B.-G.; Kim, H.-J.; Kim, K.-S.; Kim, D.-E.; Kwak, C.-K.; Byun, H.-G.; Jeong, G.-T.; Jeong, H.-S.; Kim, K. *IEEE J. Solid-State Circuits* **2006**, *41*, 122–126.
(10) (a) Mercier, R.; Malugani, J.-P.; Fahys, B.; Robert, G. *Acta Crystallogr., Sect. B* **1982**, *38*, 1887. (b) Schaefer, H.; Schaefer, G.; Weiss, A. *Z. Naturforsch., B: Anorg. Chem. Org. Chem.* **1965**, *20*, 811. (c) Jansen, M.; Henseler, U. *J. Solid State Chem.* **1992**, *99*, 110.
(11) Chondroudis, K.; Kanatzidis, M. G. *Inorg. Chem.* **1995**, *34*, 5401–5402.
(12) Mercier, R.; Malugani, J.-P.; Fahys, B.; Douglade, J.; Robert, G. *J. Solid State. Chem.* **1982**, *43*, 151.
(13) Aitken, J. A.; Canlas, C.; Weliky, D. P.; Kanatzidis, M. G. *Inorg. Chem.* **2001**, *40*, 6496.
(14) Chondroudis, K.; Kanatzidis, M. G. *Inorg. Chem.* **1998**, *37*, 2582.
(15) Chung, I.; Karst, A. L.; Weliky, D. P.; Kanatzidis, M. G. *Inorg. Chem.* **2006**, *45*, 2785–2787.
(16) Chung, I.; Do, J.; Canlas, C. G.; Weliky, D. P.; Kanatzidis, M. G. *Inorg. Chem.* **2004**, *43*, 2762–2764.
(17) (a) Kanatzidis, M. G. *Curr. Opin. Solid State Mater. Sci.* **1997**, *2*, 139–149. (b) McCarthy, T. J.; Kanatzidis, M. G. *Chem. Mater.* **1993**, *5*, 1061–1063. (c) Chan, B. C.; Hess, R. F.; Feng, P. L.; Abney, K. D.; Dorhout, P. K. *Inorg. Chem.* **2005**, *44*, 2106–2113. (d) Chen, J. H.; Dorhout, P. K.; Ostenson, J. E. *Inorg. Chem.* **1996**, *35*, 5627–5633. (e) Evenson, C. R.; Dorhout, P. K. *Inorg. Chem.* **2001**, *40*, 2875–2883. (f) Hess, R. F.; Abney, K. D.; Burris, J. L.; Hochheimer, H. D.; Dorhout, P. K. *Inorg. Chem.* **2001**, *40*, 2851–2859. (g) Piccoli, P. M. B.; Abney, K. D.; Schoonover, J. D.; Dorhout, P. K. *Inorg. Chem.* **2001**, *40*, 4871–4875.
(18) (a) Gutzmann, A.; Näther, C.; Bensch, W. *Solid State Sci.* **2004**, *6* (10), 1155–1162. (b) Gutzmann, A.; Näther, C.; Bensch, W. *Acta Crystallogr., Sect. E* **2005**, *61*, I20–I22. (c) Wu, Y. D.; Bensch, W. *Inorg. Chem.* **2007**, *46* (15), 6170–6177.
(19) (a) Komm, T.; Schleid, T. *J. Solid State Chem.* **2005**, *178* (2), 454–463. (b) Komm, T.; Schleid, T. *Z. Anorg. Allg. Chem.* **2004**, *630* (5), 712–716. (c) Schleid, T.; Hartenbach, I.; Komm, T. *Z. Anorg. Allg. Chem.* **2002**, *628* (1), 7–9.
(20) (a) Wheeler, R. A.; Whangbo, M. H.; Hughbanks, T.; Hoffmann, R.; Burdett, J. K.; Albright, T. A. *J. Am. Chem. Soc.* **1986**, *108*, 2222–2226. (b) Kunz, M.; Brown, I. D. *J. Solid State Chem.* **1995**, *115*, 395–406. (c) Hal- asyamani, P. S. *Chem. Mater.* **2004**, *16*, 3586–3592.
(21) Supporting Information.
(22) Nikogosyan, D. N. *Nonlinear optical crystals: a complete survey*; Springer-Science: New York, 2005.
(23) Crystal data for $KZrPSe_6$ at 298(2) K: Synchrotron radiation ($\lambda = 0.406\,63$ Å, $Pmc2_1$, $a = 3.7079(10)$ Å, $b = 15.074(5)$ Å, $c = 18.491(6)$ Å, $V = 1033.5(5)$ Å^3, $Z = 4$, $\rho_{calcd} = 4.080$ g/cm^3, $\mu = 5.624$ mm^{-1}, $F(000) = 1112$, $\theta = 0.77°-20.65°$, Index ranges: $-5 \le h \le 5, -22 \le k \le 23, -28 \le l \le 31$, 30 002 total reflections, 5045 independent reflection with R(int.) = 0.1827, Completeness to $\theta = 19.72°$: 95%, Refinement method: Full-matrix least-squares on F^2, Data/restraints/parameters = 5045/0/108, Refinement on F^2, GOF = 1.35, Final R indices [$I > 3\sigma(I)$]: $R_{obs} = 0.0644$, $wR_{obs} = 0.1220$. R indices (all data): $R_{all} = 0.1885$, $wR_{all} = 0.1646$. Largest diff. peak and hole = 4.18 and −4.96 e•Å^{-3}.
(24) Chondroudis, K.; Kanatzidis, M. G. *Angew. Chem., Int. Ed. Engl.* **1997**, *36*, 1324–1326.
(25) (a) Park, S.-J.; Choi, E.-S.; Oh, E.-J.; Lee, K, -W. *Synth. Met.* **2001**, *117*, 95–97. (b) Rabindranath, A. R.; Zhu, Y.; Heim, I.; Tieke, B. *Macromolecules* **2006**, *39*, 8250–8256.
(26) Canlas, C. G.; Kanatzidis, M. G.; Weliky, D. P. *Inorg. Chem.* **2003**, *42*, 3399–3405.
(27) O'Neal, S. C.; Pennington, W. T.; Kolis, J. W. *Angew. Chem., Int. Ed. Engl.* **1990**, *29*, 1486–1488.
(28) (a) Mitzi, D. B.; Kosbar, L. L.; Murray, C. E.; Copel, M.; Afzali, A. *Nature* **2004**, *428*, 299–303. (b) Mitzi, D. B.; Copel, M.; Murray, C. E. *Adv. Mater.* **2006**, *18*, 2448–2452. (c) Mitzi, D. B.; Raoux, S.; Schrott, A. G.; Copel, M.; Kellock, A.; Jordan-Sweet, J. *Chem. Mater.* **2006**, *18*, 6278–6282.
(29) (a) Kurtz, S. K.; Perry, T. T. *J. Appl. Phys.* **1968**, *39*, 3798–3813. (b) Dougherty, J. P.; Kurtz, S. K. *J. Appl. Crystallogr.* **1976**, *9*, 145–158.
(30) (a) Tsai, C.-A.; Wu, A. Y.; Liou, W.-R.; Lin, W.-C. *Jpn. J. Appl. Phys.* **2004**, *43*, 1348–1356. (b) Densiyuk, I. Y.; Burunkova, J. E. *Mol. Cryst. Liq. Cryst.* **2007**, *467*, 213–226. (c) Cui, Y.; Chen, L.; Qian, G.; Wang, M. *J. Non-Cryst. Solids* **2008**, *354*, 1211–1215.
(31) Stucky, G. D.; Phillips, M. L. F.; Gier, T. E. *Chem. Mater.* **1989**, *1*, 492–509.

JA804166M